

Supporting Information

From $M(BH_4)_3$ ($M = La, Ce$) borohydride frameworks to controllable synthesis of porous hydrides and ion conductors

Morten Brix Ley,^{a,b,*} Mathias Jørgensen^a, Radovan Černý^c, Yaroslav Filinchuk^d, and Torben R. Jensen^{a,*}

^{a)} Center for Materials Crystallography (CMC), Interdisciplinary Nanoscience Center (iNANO) and Department of Chemistry, University of Aarhus, Langelandsgade 140, DK-8000 Århus C, Denmark

^{b)} Max-Planck-Institut für Kohlenforschung, Kaiser-Wilhelm-Platz 1, 45470 Mülheim an der Ruhr, Germany

^{c)} Laboratory of Crystallography, DQMP, University of Geneva, Quai Ernest-Ansermet 24, CH-1211 Geneva, Switzerland.

^{d)} Institute of Condensed Matter and Nanosciences, Université catholique de Louvain, Place L. Pasteur 1, 1348 Louvain-la-Neuve, Belgium

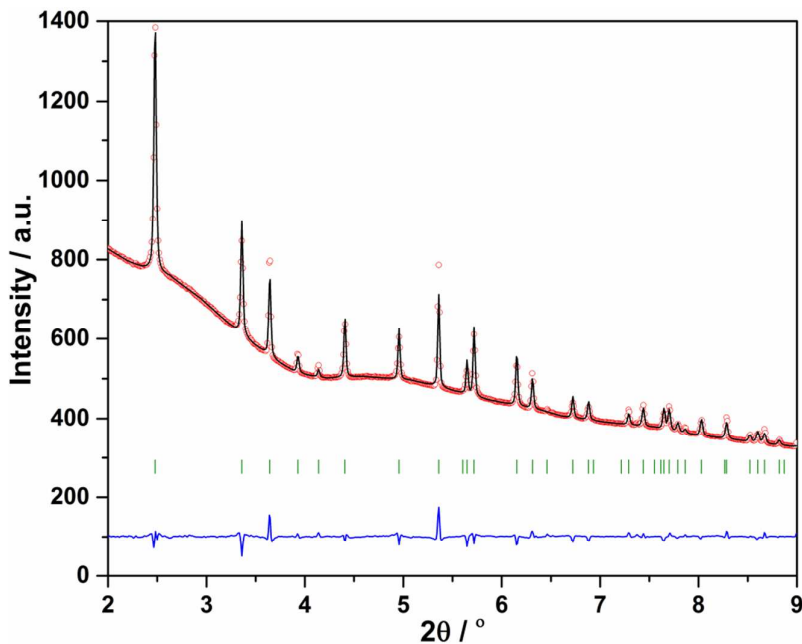


Figure S1 Rietveld refinement of SR-PXD data from $r\text{-La}(BH_4)_3$ (beam line P02.1, Petra III, DESY, $\lambda = 0.2309 \text{ \AA}$, room temperature after annealing at $T = 140 \text{ }^\circ\text{C}$). Tic marks: $r\text{-La}(BH_4)_3$.

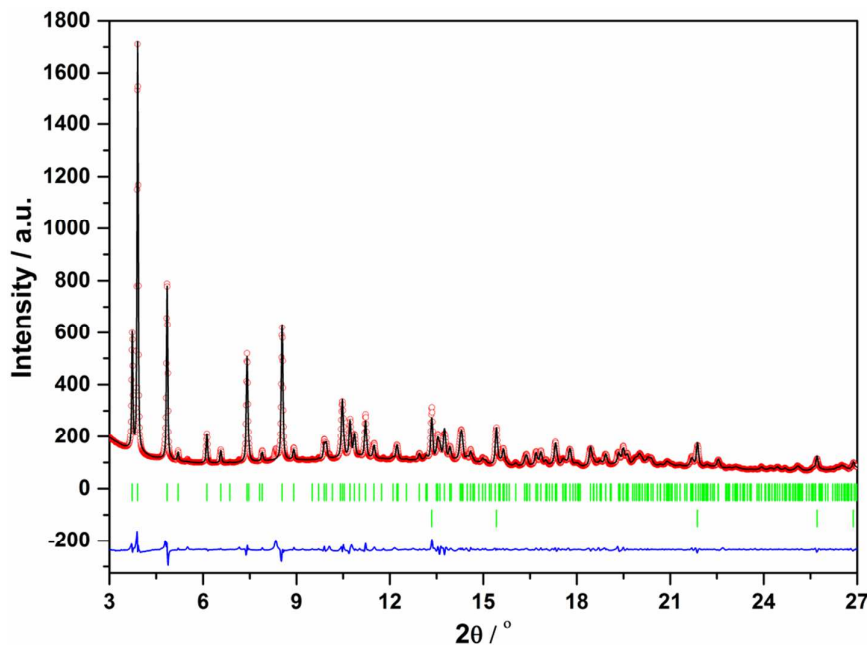


Figure S2 Le Bail refinement of the SR-PXD data obtained from $\text{LiCe}(\text{BH}_4)_3\text{Cl}\cdot n\text{Et}_2\text{O}$ (BM01A, SNBL, ESRF, $\lambda = 0.688423 \text{ \AA}$, room temperature). Tic marks: Top $\text{LiCe}(\text{BH}_4)_3\text{Cl}\cdot n\text{Et}_2\text{O}$, bottom LiCl .

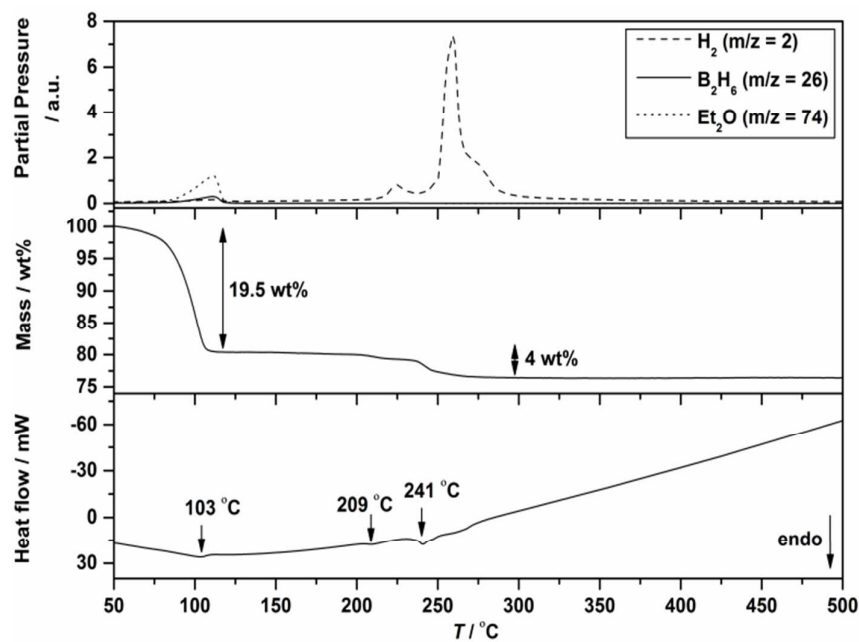


Figure S3 Thermal analysis and mass spectrometry of $\text{LiCe}(\text{BH}_4)_3\text{Cl}\cdot n\text{Et}_2\text{O}$, DSC (bottom), TGA (middle) and MS (top), $\Delta T/\Delta t = 5 \text{ }^\circ\text{C}/\text{min}$, argon flow.

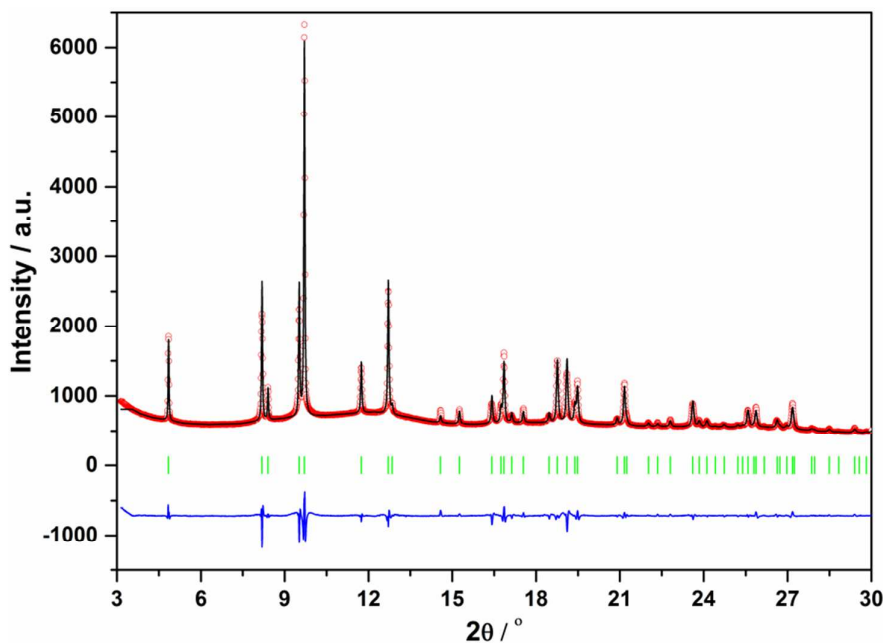


Figure S4 Le Bail refinement of the SR-PXD data obtained from $\text{La}(\text{BH}_4)_3 \cdot m\text{S}(\text{CH}_3)_2$ (I11, Diamond, $\lambda = 0.827120 \text{ \AA}$, $T = 117 \text{ }^\circ\text{C}$). Tic marks: $\text{La}(\text{BH}_4)_3 \cdot m\text{S}(\text{CH}_3)_2$.

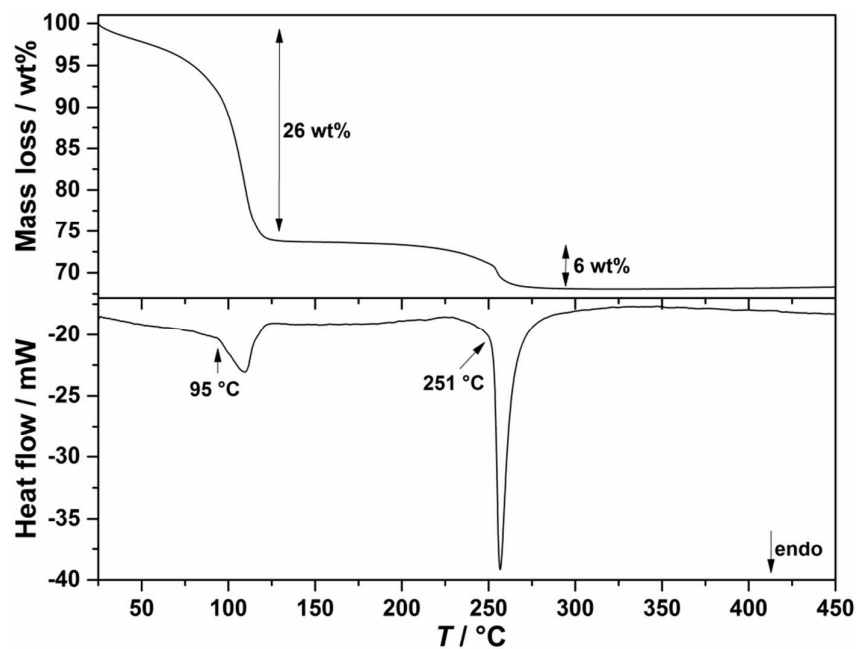


Figure S5 Thermal analysis of $\text{Ce}(\text{BH}_4)_3 \cdot n\text{S}(\text{CH}_3)_2$, DSC (bottom) and TGA (top), $\Delta T/\Delta t = 5 \text{ }^\circ\text{C}/\text{min}$, argon flow.

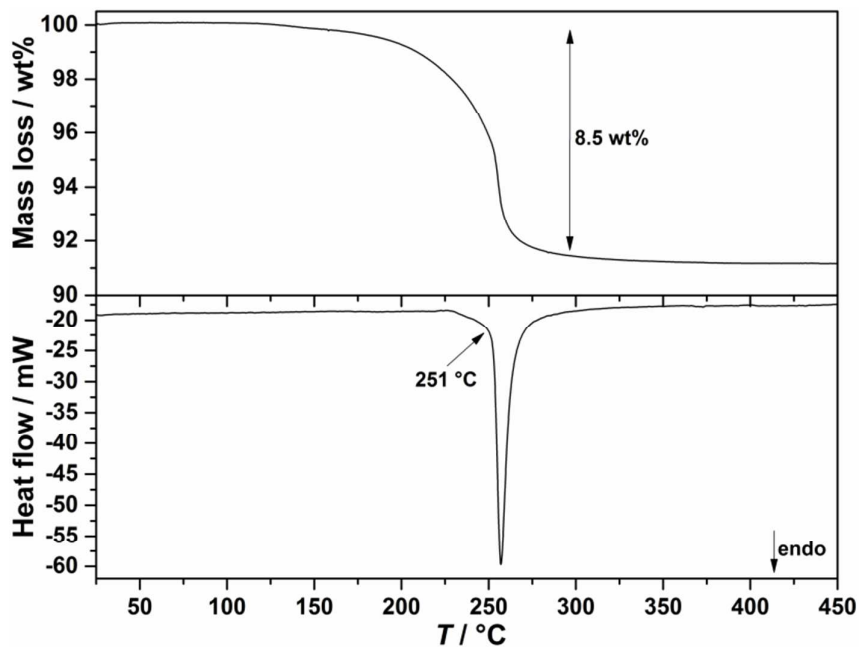


Figure S6 Thermal analysis for $\text{Ce}(\text{BH}_4)_3$, DSC (bottom) and TGA (top), from room temperature to 450 °C, $\Delta T/\Delta t = 5 \text{ }^{\circ}\text{C}/\text{min}$, argon flow.

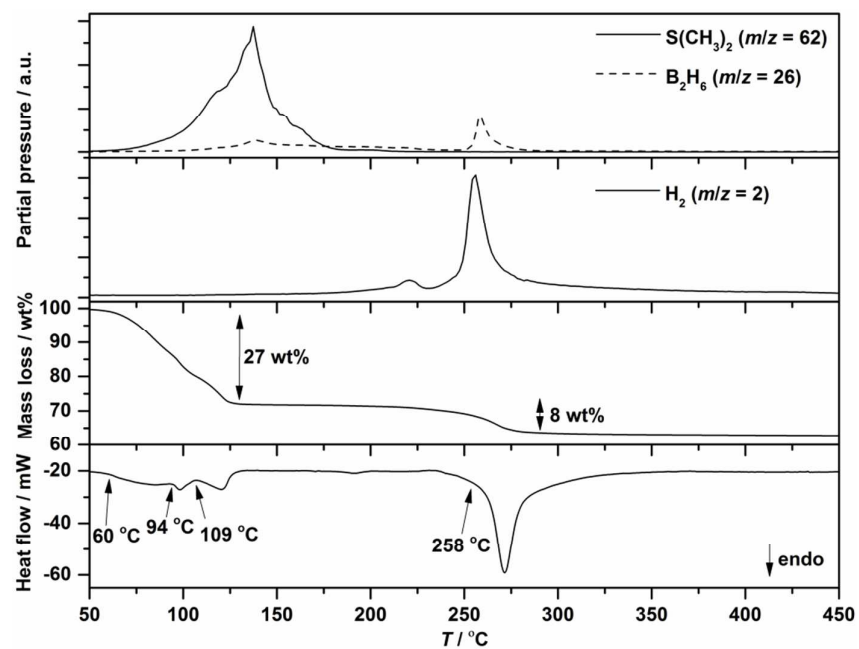


Figure S7 Thermal analysis for $\text{La}(\text{BH}_4)_3 \cdot n\text{S}(\text{CH}_3)_2$, DSC (bottom), TGA (middle) and MS (top two rows) from room temperature to 450 °C, $\Delta T/\Delta t = 5 \text{ }^{\circ}\text{C}/\text{min}$, argon flow.

Table S1 Atomic positions for *r*-Ce(BH₄)₃ (space group *R*-3*c*, *a* = 7.3745(1) Å, *c* = 20.1567(2) Å, *T* = 180 °C) determined by Rietveld refinement of the SR-PXD data.

Atom	Wyck.	x/a	y/b	z/c
Ce	6b	0	0	0
B	18e	0.632(2)	0	1/4
H1	36f	0.461(2)	-0.094(5)	0.261(2)
H2	36f	0.759(2)	0.026(5)	0.288(2)

Table S2 Atomic positions for *c*-Ce(BH₄)₃ (space group *Fm*-3*c*, *a* = 11.7106(6) Å, *T* = 180 °C) determined by Rietveld refinement of the SR-PXD data.

Atom	Wyck.	x/a	y/b	z/c
Ce	8b	0	0	0
B	24c	0	0	1/4
H1	96i	0	0.4075(1)	0.3104(1)